J. Cent. South Univ. (2015) 22: 4872−4881
DOI: 10.1007/s11771-015-3039-z

Springer

Analytical prediction and field validation of transient temperature field in asphalt pavements

CHEN Jia-qi(陈嘉祺)[1, 2], LI Liang(李亮)[1], WANG Hao(汪浩)[2]

1. School of Civil Engineering, Central South University, Changsha 410075 China;
2. Dept. of Civil and Environmental Engineering, Rutgers, The State University of New Jersey, Piscataway, NJ 08854, USA

Abstract: This work presented the development and validation of an analytical method to predict the transient temperature field in the asphalt pavement. The governing equation for heat transfer was based on heat conduction radiation and convection. An innovative time-dependent function was proposed to predict the pavement surface temperature with solar radiation and air temperature using dimensional analysis in order to simplify the complex heat exchange on the pavement surface. The parameters for the time-dependent pavement surface temperature function were obtained through the regression analysis of field measurement data. Assuming that the initial pavement temperature distribution was linear and the influence of the base course materials on the temperature of the upper asphalt layers was negligible, a close-form analytical solution of the temperature in asphalt layers was derived using Green's function. Finally, two numerical examples were presented to validate the model solutions with field temperature measurements. Analysis results show that the solution accuracy is in agreement with field data and the relative errors at a shallower depth are greater than those at a deeper one. Although the model is not sensitive to dramatic changes in climatic factors near the pavement surface, it is applicable for predicting pavement temperature field in cloudless days.

Key words: asphalt pavement; transient temperature field; heat transfer; dimensional analysis; regression analysis; Green's function

1 Introduction

As a viscoelastic material, the properties of asphalt concrete vary due to temperature changes and subsequently the stress conditions of asphalt concrete under vehicular loading are affected [1–2]. On the other hand, thermal stress could be generated in the asphalt pavement, which may cause thermal cracking when the temperature decreases [3]. Therefore, pavement temperature is one of the most important factors that need to be considered in the design and analysis of asphalt pavement.

In the natural environment, pavement structure exchanges heat with the external environment on the pavement surface, and the pavement temperature field is significantly influenced by climatic factors such as solar radiation, air temperature and wind speed [4]. Many researches were conducted on predicting pavement temperature with climatic data input. Some studies were focused on predicting the maximum temperature in the pavement using analytical methods [5–6]; while others focused on predicting pavement transient temperature fields [7–9]. YAN [10] proposed an analytical solution of temperature field in a layered pavement system with an assumption that the variations of climate factors were represented by trigonometric series. LIU and YUAN [11] presented an analytical solution of pavement temperature field in a three-layer pavement system on the basis of Fourier-Biot heat conduction equation. The statistical regression method was used by DIEFENDERFER and AL-QADI [12] to express the variation of pavement temperature when solar radiation and air temperature were known. Recently, WANG and ROESLER [13] derived an analytical solution of one-dimensional pavement temperature field through Laplace transform and inverse Laplace transform. Moreover, based on the assumption of the uniform initial pavement temperature, WANG [14] obtained an analytical solution of one-dimensional pavement temperature field with the measured pavement surface temperature.

Generally, pavement surface temperature is treated as the boundary condition in the heat conduction equation to calculate the transient temperature field

Foundation item: Project(2012zzts019) supported by the Fundamental Research Funds for the Central Universities, China; Project(201306370121) supported by State Scholarship Fund of China; Project(51248006) supported by the National Natural Science Foundation, China
Received date: 2014−12−05; **Accepted date:** 2015−04−10
Corresponding author: CHEN Jia-qi, PhD Candidate; Tel: +86–13875997701; E-mail: chenjiaqi@csu.edu.cn

within the pavement structure. In previous studies, different methods were used for estimating the pavement surface temperature. WANG and ROESLER [13] presented the analytical expression of surface boundary condition based on the conservation of energy on the pavement surface. Since heat exchange on the pavement surface is complex, some researchers developed methods to simplify the calculation model. For instance, LIU and YUAN [11] assumed that the pavement surface temperature could be expressed as a trigonometric series. WANG [14] used the measured pavement surface temperature as the boundary condition. Although these simplified methods showed reasonable accuracy, they could not reflect the influence of climatic factors on pavement temperature due to the ignorance of climatic data.

In this work, an analytical method was developed to predict the asphalt pavement temperature field using dimensional analysis, field measurements, and regression analysis. Through analyzing the relationship between climatic factors and time, an innovative time-dependent function was proposed to represent the pavement surface temperature, which was used as the boundary condition for solving the one-dimensional heat conduction problem. On the assumption that the initial pavement temperature distribution is linear and the influence of base course materials to the upper asphalt layers is negligible, a close-form analytical solution of the temperature field in the asphalt layers was obtained through the Green's function. Finally, two numerical examples were presented to validate the model solutions with field temperature measurements.

2 Establishment of prediction model for pavement temperature field

2.1 Heat transfer modes

There are three heat transfer modes (i.e., radiation, convection and conduction) in terms of the heat transfer theory. In the natural environment, pavement exchanges heat with the external environment through thermal radiation and thermal convection on the pavement surface. At the same time, pavement layers exchange heat through heat conduction.

Thermal radiation between pavement surface and the natural environment mainly includes solar radiation, atmospheric down welling long wave radiation, and radiation outgoing from the pavement surface [15]. Solar radiation and atmospheric down welling long wave radiation can increase pavement temperature, while radiation outgoing from the pavement surface will decrease pavement temperature.

Solar radiation is the main heat source for pavement. Generally, the daily solar intensity changes with time. In a cloudless day, solar radiation intensity changes from zero to positive values at the time of sunrise, reaches the peak at noon, and then gradually decreases and becomes zero at the time of sunset [16]. In this work, the daily solar radiation intensity is expressed as a function of time as

$$Q = Q(t) \tag{1}$$

where Q is the solar radiation intensity, W/m^2; $Q(t)$ is a function of time t.

The atmospheric down welling long wave radiation and radiation outgoing from the pavement surface are related to the temperature and can be expressed as Eq. (2) and Eq. (3), respectively [6].

$$q_{\mathrm{a}} = \varepsilon_{\mathrm{a}} \sigma T_{\mathrm{a}}^4 \tag{2}$$

$$q_{\mathrm{r}} = \varepsilon_{\mathrm{r}} \sigma T_{\mathrm{s}}^4 \tag{3}$$

where q_{a} is the atmospheric down welling long wave radiation, W/m^2; q_{r} is the radiation outgoing from the pavement surface, W/m^2; ε_{a} is the atmosphere emission coefficient; ε_{r} is the pavement surface emission coefficient; σ is Stefan-Boltzman constant, 5.68×10^{-8} W/(m^2·K^4); T_{a} is the air temperature, K; T_{s} is the pavement surface temperature, K.

Convective heat transfer between pavement surface and the external environment follows the Newton cooling formula [6] expressed as

$$q_{\mathrm{c}} = B \cdot (T_{\mathrm{s}} - T_{\mathrm{a}}) \tag{4}$$

where q_{c} is loss energy to the air, W/m^2; B is convective heat exchange coefficient related to the wind speed, W/(m^2·K).

The major heat transfer mode inside the pavement structure is conduction, which follows Fourier law. The governing equation for one-dimensional heat conduction model in a layered pavement can be expressed as [13]

$$\frac{\partial T_i(x,t)}{\partial t} - \alpha_i \frac{\partial^2 T_i(x,t)}{\partial x^2} = 0 \tag{5}$$

where x is the depth under the pavement surface, m; t is time, s; i represents the i-th layer of the layered pavement system; $T_i(x,t)$ represents the pavement temperature at time of t and depth of x, °C; α_i represents the thermal diffusivity of layer i, m^2/s.

Accordingly, the one-dimensional pavement temperature field can be calculated by solving Eq. (5) when proper boundary conditions and initial conditions are applied.

2.2 Dimensional analysis for pavement surface temperature

Heat exchange modes on pavement surface include radiation and convection. According to Eq. (1) to Eq. (3),

the main climatic factors that influence the radiation heat transfer on pavement surface include solar radiation intensity (Q), and air temperature (T_a). The solar radiation intensity is an instantaneous value, which is influenced by the cloud cover. When the cloud cover is considerable, the solar radiation intensity will decrease dramatically [16]. On the contrary, in a cloudless day, the influence of accidental cloud is little. If the cloud only blocks the sun for a short time, the instantaneous solar radiation intensity may drop dramatically, but it has little influence on the total amount of solar radiation since the time is very short. Therefore, the cumulative solar radiation is more stable and is used to predict the pavement surface temperature in this work. The cumulative solar radiation is defined as

$$Q_{\Delta t}=\int_{t-\Delta t}^{t}Q(t)\mathrm{d}t \tag{6}$$

where $Q_{\Delta t}$ is the cumulative solar radiation from time t–Δt to time t, J/m^2.

According to Eq. (4), the main climatic factors that influence the convection on the pavement surface include the wind speed and the air temperature. Because the variation of wind speed with time is irregular, it is impossible to import time-dependent wind speed in the analytical prediction. Therefore, wind speed is treated as a constant in this work. In addition, the convective heat exchange coefficient B can be expressed as a function of air properties (thermal conductivity, Prandtl number, and kinematic viscosity), pavement dimension, and wind speed [17]. When air properties and pavement dimension are fixed, the wind speed is the only influence factor of the convective heat exchange coefficient B. In this case, the convective heat exchange coefficient B is treated as a constant (i.e., the wind speed remains the same) in this work.

Since the solar radiation only influences the pavement surface heat exchange during the daytime, the variation of pavement temperature during the day is different from that at night. In order to identify this difference, an innovative function shown in Eq. (7) is created to express the relationship between the pavement surface temperature and the climatic factors:

$$\begin{aligned}T_s=&F_1(T_a)[H(t)-H(t-t_1)+H(t-t_2)-H(t-t_3)]+\\&F_2(Q_{\Delta t},T_a)[H(t-t_1)-H(t-t_2)]\end{aligned} \tag{7}$$

where F_1 and F_2 are undetermined functions which represent the climate-dependent variation of pavement temperature during the nighttime and daytime, respectively; t is time, h; t_1 is the sunrise time, h; t_2 is the sunset time, h; t_3 is the length of time throughout the day, 24 h; $H(t)$ is Heaviside function, which is defined as

$$H(t)=\begin{cases}1, & t>0\\0, & t<0\end{cases} \tag{8}$$

Considering the dimensions of temperature, mass and time are Θ, M, and t, respectively, the dimensions of the physical quantities in Eq. (7) are as follows: dim $T_s=\Theta$, dim $Q_{\Delta t}=MT^{-2}$, dim $T_a=\Theta$. And the dimension of the convective heat exchange coefficient B is $MT^{-3}\Theta^{-1}$. Based on the principle that the dimensions are uniform on both sides of the equation, we have

$$\begin{aligned}\dim T_s=&\dim T_a[H(t)-H(t-t_1)+H(t-t_2)-H(t-t_3)]+\\&\dim\left(\frac{Q_{\Delta t}}{\int_{t-\Delta t}^{t}B\mathrm{d}t}+T_a\right)\cdot[H(t-t_1)-H(t-t_2)]=\Theta\end{aligned} \tag{9}$$

After the dimensionless coefficients are determined, the prediction equation of pavement surface temperature is given by

$$\begin{aligned}T_s=&k_1T_a[H(t)-H(t-t_1)+H(t-t_2)-H(t-t_3)]+\\&\left(k_2\frac{Q_{\Delta t}}{\int_{t-\Delta t}^{t}B\mathrm{d}t}+k_3T_{a1}\right)[H(t-t_1)-H(t-t_2)]\end{aligned} \tag{10}$$

where k_1, k_2 and k_3 are the coefficients, which are dimensionless; T_{a1} is the air temperature at a certain time, °C.

At $t=t_1$, the solar radiation starts to influence the pavement surface temperature, and meanwhile the value of cumulative solar radiation is still zero. In order to ensure the continuity of Eq. (10), the values of $k_3\cdot T_{a1}$ should be equal to $k_1\cdot T_a$ at $t=t_1$. Therefore, T_{a1} represents the air temperature at the time of t_1, and $k_3=k_1$. Thus, Eq. (10) can be reduced to Eq. (11) as

$$\begin{aligned}T_s=&k_1T_a[H(t)-H(t-t_1)+H(t-t_2)-H(t-t_3)]+\\&\left(k_2\frac{Q_{\Delta t}}{B_{\Delta t}}+k_1T_{a(t=t_1)}\right)[H(t-t_1)-H(t-t_2)]\end{aligned} \tag{11}$$

where $B_{\Delta t}$ is the definite integral of B from the time of t–Δt to the time of t, namely, $\int_{t-\Delta t}^{t}B\mathrm{d}t$, J/(m^2·ºC).

2.3 Parameter determination with field data and regression analysis

In order to obtain the parameters of k_1, k_2 in Eq. (11) and validate the prediction model of pavement surface temperature, field test was conducted to measure the related data, including pavement surface temperature, pavement temperature at different depths, cumulative solar radiation, and air temperature.

The field test site locates at the G225 highway (109.8° east longitude, and 19.8° north latitude) in Hainan Province of China. The pavement structure is listed in Table 1. The annual average temperature varies from 24.2 ºC to 25.0 ºC and the local annual average wind speed varies from 1.5 m/s to 2.5 m/s, respectively. The annual total solar radiation is about 5790 MJ/m^2.

Three pavement cross-sections were included in the

Table 1 Pavement structure pattern

Layer No.	Material variation	Thickness/cm
1	Asphalt concrete (AC-13)	4
2	Asphalt concrete (AC-20)	8
3	Modified graded gravel	15
4	Cement stabilized crushed stone	30
5	Soil	—

field measurement. For each cross-section, seven platinum resistance temperature sensors (with a range of 0–80 ºC and the accuracy of ±0.5 ºC) were used to measure the pavement temperature at different depths, and the TBQ-2 solar radiation intensity meter (with a range of 0–2000 W/m^2 and the accuracy of ±2%) was used to measure the cumulative solar radiation. The measured data were automatically stored once every 5 min and 10 min for temperature and cumulative solar radiation, respectively. The depths of the temperature sensors were at 0 (pavement surface), 4, 6, 8, 10 and 12 cm from the pavement surface.

The cumulative solar radiation $Q_{\Delta t}$ can be measured in the field test. CHEN et al [18] analyzed the correlation between cumulative solar radiation and pavement surface temperature when the cumulative time (Δt in Eq. (6)) changes, and found that the maximum correlation coefficient could be reached when Δt=4 h. Therefore, the Δt=4 h was used in this work. Since the wind speed is assumed to be constant in this work, $B_{\Delta t}$ is only related to Δt, and is a constant for Δt=4 h. When the wind speed is equal to the average wind speed (i.e. 2 m/s) in the field test site, the convective heat exchange coefficient B is equal to 12.9 W/(m^2·ºC) [19]. Accordingly, $B_{\Delta t}$ is 1.9× 105 J/(m^2·ºC).

Based on Eq. (11), the values of parameters k_1 and k_2 can be obtained through field test and regression analysis. According to the field test results from July, 2011 to February, 2012, the values of k_1, k_2 were valued as 1.13 and 0.28 respectively in cloudless days.

3 Derivation of analytical solutions

The temperature inside the pavement structure is not directly influenced by the external environment. Different parts of pavement structure exchange heat through heat conduction. Neglecting the heat transfer in the horizontal direction of the pavement, the governing equation for one-dimensional heat conduction model in a layered pavement can be expressed by Eq. (5). The interlayer thermal contact conditions and different thermophysical parameters for each layer are needed for solving Eq. (5). Therefore, the explicit expression of pavement temperature has not been obtained in previous studies.

Previous studies showed that the thermal properties of base course materials influence the base course temperature obviously, but have little effect on the temperature of the upper surface courses [10]. Compared with base course materials, thermal properties of asphalt layers have controlling impact on temperature field in the asphalt layer. Since this work is focused on the temperature field of asphalt layer but not base course, the difference in thermal properties of base materials is neglected to simplify the model. This simplification is proved to be acceptable after the calculated temperature is validated with the measured data presented in the next section. On the basis of the above assumption, the governing equation for one-dimensional heat conduction model is given by

$$\frac{\partial T(x,t)}{\partial t}-\alpha\frac{\partial^2 T(x,t)}{\partial x^2}=0 \tag{12}$$

The boundary conditions and the initial condition can be given by

$$T(0,t)=f(t) \tag{13}$$

$$T(l,t)=g(t) \tag{14}$$

$$T(x,0)=\varphi(x) \tag{15}$$

where $f(t)$ represents pavement surface temperature varying with time; $g(t)$ represents the pavement temperature at the depth of l varying with time; $\varphi(x)$ represents the pavement temperature varying with the depth x for t=0.

Given the following partial differential equation as

$$\frac{\partial T(x,t)}{\partial t}-\alpha\frac{\partial^2 T(x,t)}{\partial x^2}=F(x,t) \tag{16}$$

and combining the conditions (Eq. (13)–Eq. (15)), the solution of Eq. (16) can be obtained through Green's function and variable separation method as

$$T(x,t)=\int_0^l G(x,t;\xi,0)\varphi(\xi)\mathrm{d}\xi+\int_0^t \mathrm{d}\tau\int_0^l G(x,t;\xi,\tau)\cdot F(\xi,\tau)\mathrm{d}\xi+\alpha\int_0^t[G_\xi(x,t;0,\tau)f(\tau)-G_\xi(x,t;l,\tau)g(\tau)]\mathrm{d}\tau \tag{17}$$

where G represents Green's function and G_ξ represents the partial derivative of ξ in Green's function, expressed as

$$G(x,t;\xi,\tau)=\sum_{n=1}^{\infty}\frac{2}{l}\sin\frac{n\pi\xi}{l}\sin\frac{n\pi x}{l}\mathrm{e}^{-(\frac{n\pi}{l})^2\alpha(t-\tau)} \tag{18}$$

$$G_\xi(x,t;\xi,\tau)=\sum_{n=1}^{\infty}\frac{2n\pi}{l^2}\cos\frac{n\pi\xi}{l}\sin\frac{n\pi x}{l}\mathrm{e}^{-(\frac{n\pi}{l})^2\alpha(t-\tau)} \tag{19}$$

Equation (17) gives the general form solution for the heat transfer model and can be found in some heat

transfer textbooks [20]. However, in order to apply it in pavement temperature prediction, two issues should be solved. First, the detailed functions of boundary and initial conditions should be established. These functions should actually reflect the pavement heat transfer conditions. Second, it should be ensured that when the detailed functions of boundary and initial conditions are applied, Eq. (17) can be solved, and the detailed solution should be derived. These issues are solved by the authors in the following sections.

For the one-dimensional heat transfer model, $F(x,t)\equiv 0$. Thus, Eq. (17) can be simplified as

$$T(x,t)=\int_0^l G(x,t;\xi,0)\varphi(\xi)\mathrm{d}\xi+\alpha\int_0^t[G_\xi(x,t;0,\tau)f(\tau)-G_\xi(x,t;l,\tau)g(\tau)]\mathrm{d}\tau \quad (20)$$

Before calculating Eq. (20), Eq. (13) to Eq. (15) should be determined first.

According to the field test, the variation of $Q_{\Delta t}$ (Δt=4 h) in a cloudless day is shown in Fig. 1.

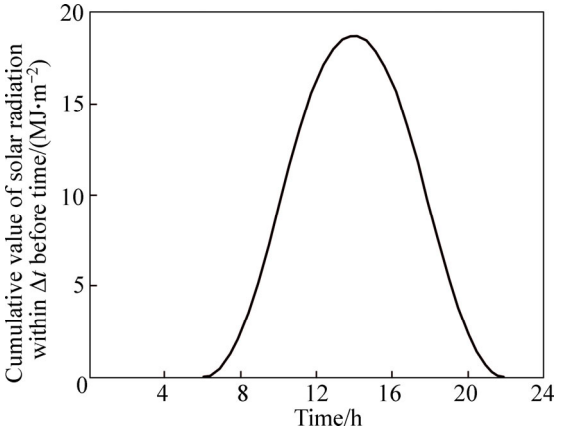

Fig. 1 Variation of cumulative value of solar radiation in a cloudless day

The variation of $Q_{\Delta t}$ can be expressed with a function that is similar to the normal distribution function, expressed as [18]

$$Q_{\Delta t}=a\cdot \mathrm{e}^{-\frac{(t-b)^2}{c^2}} \quad (21)$$

where a, b and c are parameters needed to be determined.

During most of time at night, the cumulative solar radiation value is zero (Fig. 1). However, the function shown in Eq. (21) is greater than zero during the whole day, which is inconsistent with the actual situation. Moreover, since Eq. (21) is not a periodic function, the periodic variation of solar radiation cannot be simulated. Therefore, the variation of $Q_{\Delta t}$ with time is expressed with a half-sine function, and Heaviside functions are used to ensure $Q_{\Delta t}$ to be zero during a certain period. This function is expressed as

$$Q_{\Delta t}=A\sin\omega(t-t_1)[H(t-t_1)-H(t-t_2-\Delta t)] \quad (22)$$

where A is the peak value of the cumulative solar radiation, which is theoretically equal to the cumulative solar radiation when t=0.5(t_1+t_2+Δt), J·m^{-2}; ω is angular frequency and $\omega=2\pi/[2(t_2+\Delta t-t_1)]=\pi/(t_2+\Delta t-t_1)$.

According to field test results, the variations of air temperature T_a with time are shown in Fig. 2 and Fig. 3.

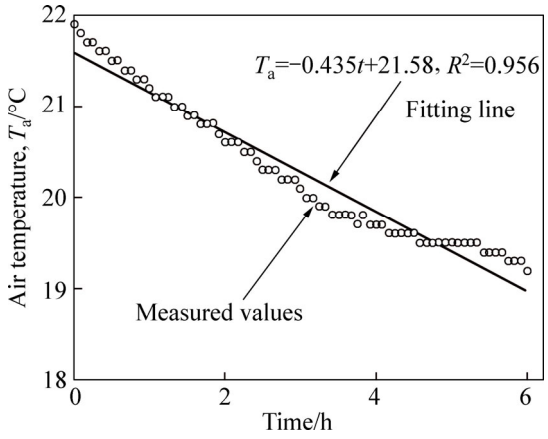

Fig. 2 A typical variation of air temperature with time ($0<t<t_1$)

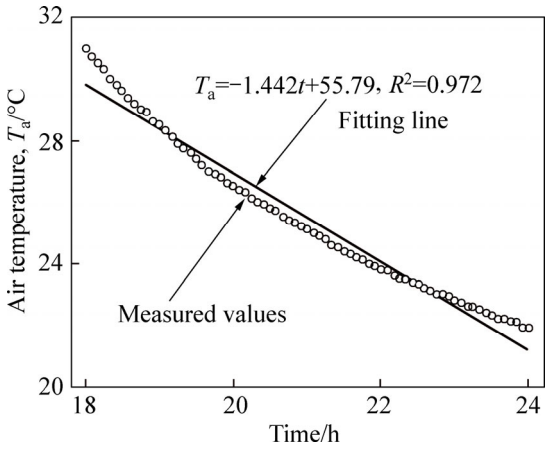

Fig. 3 A typical variation of air temperature with time ($t_2<t<t_3$)

According to Fig. 2 and Fig. 3, during the time periods of t–t_1 and t_2–t_3, the air temperature can be expressed as linear functions of time. However, the parameters are different in each period. Based on the regularity mentioned above, Eq. (23) and Eq. (24) are used to simulate the relationships between air temperature and time in different periods.

$$T_a(0\le t<t_1)=k_4t+b_1 \quad (23)$$

$$T_a(t_2\le t<t_3)=k_5t+b_2 \quad (24)$$

where k_4, k_5, b_1 and b_2 are parameters.

Substituting Eq. (22) to Eq. (24) into Eq. (11), the variation of pavement surface temperature with time can be obtained. Considering $[H(t-t_1)-H(t-t_2-\Delta t)]\cdot[H(t-t_1)-H(t-t_2)]=[H(t-t_1)-H(t-t_2)]$, the boundary condition in Eq. (13) can be expressed as

$$f(t)=T(0,t)=k_1(k_4t+b_1)[H(t)-H(t-t_1)]+$$

$$[\frac{k_2}{B_{\Delta t}}A\sin[\omega(t-t_1)]+k_1T_{a(t=t_1)}]\cdot$$
$$k_1(k_5t+b_2)[H(t-t_2)-H(t-t_3)]+$$
$$[H(t-t_1)-H(t-t_2)] \quad (25)$$

With the increasing of depth, the influence of the natural environment to the pavement temperature decreases, and the pavement temperature becomes more stable. Therefore, at a certain depth (critical depth), the road structure (not necessarily asphalt layer) temperature can be treated as constant within a day [14]. It is assumed that the depth l in Eq. (14) is the critical depth, and the boundary condition in Eq. (14) can be given by

$$g(t)=T(l,t)=T_l \quad (26)$$

where T_l is the constant temperature at the critical depth of l, °C.

According to Eq. (15), pavement temperature at t=0 should be expressed as a function of depth. The field test shows that the variation of pavement temperature with depth is approximately linear at t=0. It demonstrates that the assumption of expressing Eq. (15) with linear functions is reasonable. Accordingly, by combining Eq. (25) and Eq. (26), Eq. (15) can be expressed as

$$\varphi(x)=T(x,0)=T(0,0)+\frac{x}{l}[T(l,0)-T(0,0)]$$
$$=k_1b_1+\frac{x}{l}(T_l-k_1b_1) \quad (27)$$

All the boundary conditions and initial conditions required to solve Eq. (12) have been determined (i.e. Eq. (25) to Eq. (27)). Here, three equations are introduced as

$$T_1(x,t)=\int_0^l G(x,t;\xi,0)\varphi(\xi)\mathrm{d}\xi \quad (28)$$

$$T_2(x,t)=\alpha\int_0^t G_{\xi}(x,t;0,\tau)f(\tau)\mathrm{d}\tau \quad (29)$$

$$T_3(x,t)=\alpha\int_0^t G_{\xi}(x,t;l,\tau)g(\tau)\mathrm{d}\tau \quad (30)$$

Thus, Eq. (20) can be expressed by

$$T(x,t)=T_1(x,t)+T_2(x,t)-T_3(x,t) \quad (31)$$

Substituting Eq. (18) and Eq. (27) into Eq. (28), Eq. (28) can be expressed by

$$T_1(x,t)=\sum_{n=1}^{\infty}\frac{2}{n\pi}\mathrm{e}^{-(\frac{n\pi}{l})^2\alpha t}\sin\frac{n\pi x}{l}(k_1b_1-T_l\cos(n\pi)) \quad (32)$$

Substituting Eq. (19) and Eq. (25) into Eq. (29), Eq. (29) can be expressed as Eq. (33) for $0\le t<t_1$.

$$T_2(x,t)=\alpha\int_0^t\sum_{n=1}^{\infty}\frac{2n\pi}{l^2}\sin\frac{n\pi x}{l}\mathrm{e}^{-(\frac{n\pi}{l})^2\alpha(t-\tau)}(k_1k_4\tau+k_1b_1)\mathrm{d}\tau \quad (33)$$

For $t_1\le t<t_2$, Eq. (29) can be expressed by

$$T_2(x,t)=\alpha\int_0^{t_1}\sum_{n=1}^{\infty}\frac{2n\pi}{l^2}\sin\frac{n\pi x}{l}\mathrm{e}^{-(\frac{n\pi}{l})^2\alpha(t-\tau)}\cdot$$
$$(k_1k_4\tau+k_1b_1)\mathrm{d}\tau+\alpha\int_{t_1}^t\sum_{n=1}^{\infty}\frac{2n\pi}{l^2}\cdot$$
$$\sin\frac{n\pi x}{l}\mathrm{e}^{-(\frac{n\pi}{l})^2\alpha(t-\tau)}[\frac{k_2}{B_{\Delta t}}A\sin[\omega(\tau-t_1)]+$$
$$k_1T_{a(t=t_1)}]\mathrm{d}\tau \quad (34)$$

For $t_2\le t<t_3$, Eq. (29) can be expressed by

$$T_2(x,t)=\alpha\int_0^{t_1}\sum_{n=1}^{\infty}\frac{2n\pi}{l^2}\sin\frac{n\pi x}{l}\mathrm{e}^{-(\frac{n\pi}{l})^2\alpha(t-\tau)}\cdot$$
$$k_1k_4\tau+k_1b_1)\mathrm{d}\tau+\alpha\int_{t_1}^{t_2}\sum_{n=1}^{\infty}\frac{2n\pi}{l^2}\cdot$$
$$\sin\frac{n\pi x}{l}\mathrm{e}^{-(\frac{n\pi}{l})^2\alpha(t-\tau)}[\frac{k_2}{B_{\Delta t}}A\sin[\omega(\tau-t_1)]+$$
$$k_1T_{\mathrm{a}}(t=t_1)]\mathrm{d}\tau+\alpha\int_{t_2}^t\sum_{n=1}^{\infty}\frac{2n\pi}{l^2}\sin\frac{n\pi x}{l}\cdot$$
$$\mathrm{e}^{-(\frac{n\pi}{l})^2\alpha(t-\tau)}(k_1k_5\tau+k_1b_2)\mathrm{d}\tau \quad (35)$$

Therefore, the expression of $T_2(x,t)$ during different time periods can be expressed as follows:

For $0\le t<t_1$,

$$T_2(x,t)=\sum_{n=1}^{\infty}\frac{2}{\alpha n^3\pi^3}\sin\frac{n\pi x}{l}[(\alpha k_1b_1n^2\pi^2-k_1k_4l^2)\cdot$$
$$(1-\mathrm{e}^{-\frac{n^2\pi^2}{l^2}\alpha t})+\alpha k_1k_4n^2\pi^2t] \quad (36)$$

For $t_1\le t<t_2$,

$$T_2(x,t)=T_{21}(x,t)+\sum_{n=1}^{\infty}\frac{2}{n\pi}\sin\frac{n\pi x}{l}\{k_1T_{a(t=t_1)}\cdot$$
$$[1-\mathrm{e}^{(\frac{n\pi}{l})^2\alpha(t_1-t)}]-\frac{\alpha Ak_2n^2\pi^2}{B_{\Delta t}(\alpha^2n^4\pi^4+l^4\omega^2)}\cdot$$
$$[-l\omega^2\mathrm{e}^{(\frac{n\pi}{l})^2\alpha(t_1-t)}+l^2\omega\cos(\omega(t_1-t))+$$
$$\alpha n^2\pi^2\sin(\omega(t_1-t))]\} \quad (37)$$

where

$$T_{21}(x,t)=\sum_{n=1}^{\infty}\frac{2}{\alpha n^3\pi^3}\mathrm{e}^{-(\frac{n\pi}{l})^2\alpha t}\sin\frac{n\pi x}{l}[(k_1k_4l^2-$$
$$\alpha k_1b_1n^2\pi^2)(1-\mathrm{e}^{(\frac{n\pi}{l})^2\alpha t_1})+$$
$$\alpha k_1k_4n^2\pi^2t_1\mathrm{e}^{(\frac{n\pi}{l})^2\alpha t_1}] \quad (38)$$

For $t_2\le t<t_3$,

$$T_2(x,t)=T_{21}(x,t)+T_{22}(x,t)+\sum_{n=1}^{\infty}\frac{2}{\alpha n^3\pi^3}\sin\frac{n\pi x}{l}\cdot$$

$$\{(\alpha k_1 b_1 n^2\pi^2 - k_1 k_5 l^2)[1-\mathrm{e}^{(\frac{n\pi}{l})^2\alpha(t_2-t)}]+ \alpha k_1 k_5 n^2\pi^2[t-t_2\mathrm{e}^{(\frac{n\pi}{l})^2\alpha(t_2-t)}]\} \quad (39)$$

where

$$T_{22}(x,t)=\sum_{n=1}^{\infty}\frac{2}{n\pi}\sin\frac{n\pi x}{l}\{k_1 T_{a(t=t_1)}[\mathrm{e}^{(\frac{n\pi}{l})^2\alpha(t_2-t)}- \mathrm{e}^{(\frac{n\pi}{l})^2\alpha(t_1-t)}]+\frac{\alpha A k_2 n^2\pi^2}{B_{\Delta t}(\alpha^2 n^4\pi^4+l^4\omega^2)}\cdot [l^2\omega\mathrm{e}^{(\frac{n\pi}{l})^2\alpha(t_1-t)}-(l^2\omega\cos\omega(t_1-t_2)- \alpha n^2\pi^2\sin(\omega(t_1-t_2)))\mathrm{e}^{(\frac{n\pi}{l})^2\alpha(t_2-t)}]\} \quad (40)$$

Substituting Eq. (19) and Eq. (26) into Eq. (30), Eq. (30) can be expressed by

$$T_3(x,t)=\sum_{n=1}^{\infty}\frac{2T_l}{n\pi}\cos(n\pi)\sin\frac{n\pi x}{l}[1-\mathrm{e}^{-(\frac{n\pi}{l})^2\alpha t}] \quad (41)$$

Thus, substituting Eq. (32) and Eq. (36) to Eq. (41) into Eq. (31), the analytical solution of pavement temperature field can be obtained.

4 Model validations with field measurements

The developed solution method and calculation results were compared with field measurements for model validation. The air temperature and solar radiation collected on August 6, 2011 and November 13, 2011 was taken for analysis. Parameters needed in the calculation of pavement temperature on surface and at various depths are listed in Table 2 and Table 3.

The pavement surface temperature was calculated using Eq. (11) and the calculated temperature values were compared with the measured values, as shown in Fig. 4(a). The calculated and measured pavement temperatures at different depths are shown in Figs. 4(b)–(f).

Table 2 Parameters for calculating pavement surface temperature

Parameter	Date	Value	Source
$B_{\Delta t}$/(MJ·m^{-2}·ºC^{-1})	—	0.19	Ref. [18]
k_1	—	1.13	Regression
k_2	—	0.28	Rregression
t_1/h	2011–08–06	6.8	Field test
t_1/h	2011–11–13	7	Field test
t_2/h	2011–08–06	18	Field test
t_2/h	2011–11–13	17.7	Field test

Table 3 Parameters for calculating pavement temperature at various depths

Parameter	Date	Value	Source
α/(m^2·s^{-1})	—	0.0021	Ref. [14]
b_1	2011–08–06	29.5	Field test
b_1	2011–11–13	21.6	Field test
b_2	2011–08–06	50.6	Field test
b_2	2011–11–13	52.7	Field test
k_4	2011–08–06	-0.52	Field test
k_4	2011–11–13	-0.4	Field test
k_5	2011–08–06	-0.94	Field test
k_5	2011–11–13	-1.3	Field test
A	2011–08–06	18.7	Field test
A	2011–11–13	13.8	Field test
T_l/ºC	2011–08–06	28	Ref. [21]
T_l/ºC	2011–11–13	26	Ref. [21]

The relative errors between the calculated and measured pavement surface temperatures are listed in Table 4 in terms of the maximum relative errors and the average relative errors. It can be seen from Table 4 that the maximum relative errors in the two examples are 8.84% (total error 3.8 ºC) and 5.68% (total error 1.3 ºC), respectively, and the average relative errors are 1.93% and 1.91%, respectively. This indicates that the predicted pavement surface temperature in each time period (0–t_1, t_1–t_2, t_2–t_3) is in agreement with field measurements.

The calculated and measured pavement temperatures at different depths are shown in Figs. 4(b)–(f). It can be seen from Fig. 4(b) to Fig. 4(f) that the calculated pavement temperature profile is segmented for any given depth because the pavement surface temperature is expressed as a piecewise function. Therefore, selecting a proper function such as Eq. (25) to express the variation of pavement surface temperature with time is very important to ensure calculation accuracy of pavement temperature at given depths. Moreover, since the pavement temperature profiles are segmented, at the junctions of different periods, such as t_1 and t_2 in this work, the fluctuation of calculated temperature is relatively obvious. However, this fluctuation becomes negligible with the increasing of depth. This is because the pavement temperature at a deeper depth is not influenced by the solar radiation directly; therefore, the segmented feature of the temperature profile at a deeper depth is not observed.

The results in Figs. 4(b)–(f) show that for the temperature data on August 6, the maximum temperature at the depth of 4 cm was observed at 14:00–14:30, while the maximum temperature at the depth of 12 cm was observed at 16:00–17:00. The similar trend was observed

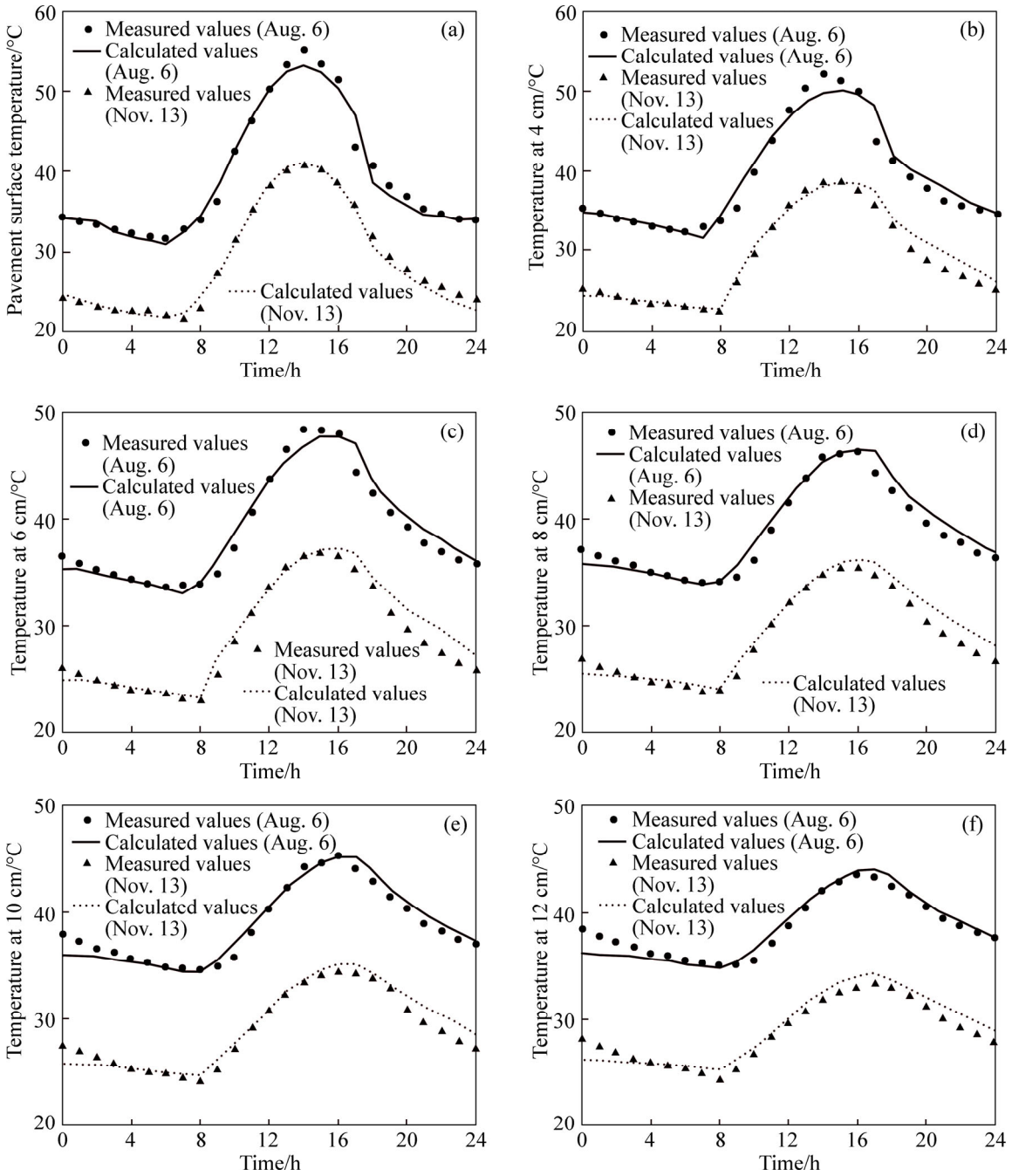

Fig. 4 Calculated and measured pavement temperatures: (a) Surface; (b) 4 cm; (c) 6 cm; (d) 8 cm; (e) 10 cm; (f) 12 cm

Table 4 Relative errors of pavement surface temperatures

Date	Time	Maximum relative error/%	Average relative error/%
2011–08–06	0:00–7:00	2.52	1.31
2011–08–06	7:00–18:00	8.84	2.55
2011–08–06	18:00–24:00	4.19	1.85
2011–08–06	0:00–24:00	8.84	1.93
2011–11–13	0:00–7:00	3.24	1.54
2011–11–13	7:00–18:00	5.68	1.40
2011–11–13	18:00–24:00	4.88	3.70
2011–11–13	0:00–24:00	5.68	1.91

for the temperature data on November 13. It indicates that the heat transfer process needs a period of time, which causes the delay of the maximum temperature at a deeper depth. This trend is captured by the model presented in this work.

The maximum and average relative errors between calculated and measured temperatures at different depths are compared in Table 5.

It can be seen that the results calculated from the developed analytical method agree well with field measurements. For both cases, the maximum relative errors between the measured and calculated temperatures

Table 5 Relative errors of pavement temperatures

Date	Depth/cm	Maximum relative error/%	Average relative error/%
2011–08–06	4	7.1	2.3
2011–08–06	6	6.3	2.0
2011–08–06	8	4.7	1.9
2011–08–06	10	3.3	1.6
2011–08–06	12	2.6	1.6
2011–11–13	4	8.0	2.9
2011–11–13	6	7.6	2.8
2011–11–13	8	6.9	2.9
2011–11–13	10	5.6	2.6
2011–11–13	12	4.1	2.8

range from 2.6% to 8.0% (total error 2.3 ºC), and the average relative errors range from 1.6% to 2.9%. This result shows that the assumptions in this work are acceptable for predicting temperature field in asphalt layer. Compared with the temperature at deeper depths, the relative temperature errors at the depth of 4 cm are greater. This is reasonable because the natural environment has a greater influence on the temperature in the upper pavement layer, which makes the pavement temperature vary more irregularly due to accidental change of climatic factors.

5 Conclusions

This work presents an analytical method for predicting the asphalt pavement temperature field with measured climatic data. An innovative model is established for predicting the asphalt pavement surface temperature through dimensional analysis, field tests and regression analysis. By analyzing the variation characteristics of solar radiation and air temperature with time, the variation of pavement surface temperature within a day is expressed as a function of time, which is used as boundary condition for solving the pavement temperature model. Based on the assumption that the influence of the temperature field in the upper asphalt layer on the base course materials can be neglected, a close-form solution is obtained based on the Green's function. Finally, the developed method is validated using field measurements and the comparisons between the calculated and the measured temperatures show good agreements.

The introduction of the pavement surface temperature in the proposed time-dependent function simplified the complex heat exchange conditions on the pavement surface. The dimensions are consistent in the governing equation of the pavement surface temperature prediction model, which ensures a clear physical meaning to understand the model. Moreover, the derived solution of pavement temperature is explicit and can be easily implemented. Field validation shows that selecting a proper function to represent the pavement surface temperature is critical to ensure the calculation accuracy of pavement temperature at given depths. The relative temperature errors at a shallower depth are greater than those at a deeper one because the natural environment has greater influence on the temperature in the upper pavement layer.

Although the developed analytical method cannot make a rapid response to the irregular dramatic changes in climatic factors, the method is useful in predicting pavement temperature with given climatic data. Therefore, it can be used to analyze the variation of pavement temperature according to the variation of climatic factors throughout the year, and predict the effect of certain climatic factors on pavement temperature.

References

[1] AIGNER E, LACKNER, R, PICHLER C. Multiscale prediction of viscoelastic properties of asphalt concrete [J]. Journal of Materials in Civil Engineering, 2009, 21(12): 771–780.

[2] WANG H, AL-QADI I L. Importance of nonlinear anisotropic modeling of granular base for predicting maximum viscoelastic pavement responses under moving vehicular loading [J]. Journal of Engineering Mechanics, 2013, 139(1): 29–38.

[3] DAVE E V, BUTTLAR W G. Thermal reflective cracking of asphalt concrete overlays [J]. International Journal of Pavement Engineering, 2010, 11(6): 477–488.

[4] HERMANSSON A. Simulation model for calculating pavement temperature including maximum temperature [J]. Transportation Research Record: Journal of the Transportation Research Board, 2000, 1699: 134–141.

[5] BARBER E S. Calculation of maximum pavement temperatures from weather reports [J]. Highway Research Board Bulletin, 1957, 168: 1–8.

[6] SOLAIMANIAN M, KENNEDY T W. Predicting maximum pavement surface temperature using maximum air temperature and hourly solar radiation [J]. Transportation Research Record: Journal of the Transportation Research Board, 1993, 1417: 1–11.

[7] MINHOTO M J C, PAIS J, PEREIRA P A A, PICADO-SANTOS L G. Predicting asphalt pavement temperature with a three-dimensional finite element method [J]. Transportation Research Record: Journal of the Transportation Research Board, 2005, 1919: 96–110.

[8] YAVUZTURK C, KSAIBATI K, CHIASSON A D. Assessment of temperature fluctuations in asphalt pavements due to thermal environmental conditions using a two dimensional transient finite-difference approach [J]. Journal of Materials in Civil Engineering, 2005, 17(4): 465–475.

[9] QIN Jian, SUN Li-jun. Study on asphalt pavement temperature field distribution pattern [J]. Journal of Highway and Transportation Research and Development, 2006, 23(8): 18–21. (in Chinese)

[10] YAN Zuo-ren. Analysis of the temperature field in layered pavement system [J]. Journal of Tongji University, 1984, 12(3): 76–85. (in Chinese)

[11] LIU C, YUAN D. Temperature distribution in layered road structures [J]. Journal of Transportation Engineering, 2000, 126(1): 93–95.

[12] DIEFENDERFER B K, AL-QADI I L, DIEFENDERFER S D. Model to predict pavement temperature profile: development and validation [J]. Journal of Transportation Engineering, 2006, 132(2): 162–167.

[13] WANG D, ROESLER J R. One-dimensional rigid pavement temperature prediction using Laplace transformation [J]. Journal of Transportation Engineering, 2012, 138(9): 1171–1177.

[14] WANG D. Analytical approach to predict temperature profile in a multilayered pavement system based on measured surface temperature data [J]. Journal of Transportation Engineering, 2012, 138(5): 674–679.

[15] HERMANSSON A. Mathematical model for paved surface summer and winter temperature: Comparison of calculated and measured temperatures [J]. Cold Regions Science and Technology, 2004, 40(1): 1–17.

[16] MATUSZKO D. Influence of the extent and genera of cloud cover on solar radiation intensity [J]. International Journal of Climatology, 2012, 32(15): 2403–2414.

[17] GUI J, PHELAN P, KALOUSH K E, GOLDEN J. Impact of pavement thermophysical properties on surface temperatures [J]. Journal of Materials in Civil Engineering, 2007, 19(8): 683–690.

[18] CHEN Jia-qi, LUO Su-ping, LI Liang, DAN Han-cheng, ZHAO Lian-heng. Temperature distribution and method-experience prediction model of asphalt pavement [J]. Journal of Central South University Science and Technology, 2013, 44(4): 1647–1656. (in Chinese)

[19] QIN Y, HILLER J E. Ways of formulating wind speed in heat convection significantly influencing pavement temperature prediction [J]. Heat and Mass Transfer, 2013, 49(5): 745–752.

[20] HAHN D W, OZISIK M N. Heat conduction [M]. 3rded. Hoboken, New Jersey: John Wiley & Sons Inc, 2012: 681–684.

[21] XING Xu-huang. The relationship between the TC frequency affecting Hainan and the variation of soil temperature in Hainan [J]. Guangdong Meteorology, 2005, 26(4): 7–10. (in Chinese)

(Edited by DENG Lü-xiang)